



PERGAMON

Journal of Quantitative Spectroscopy &
Radiative Transfer 79–80 (2003) 1159–1169

Journal of
Quantitative
Spectroscopy &
Radiative
Transfer

www.elsevier.com/locate/jqsrt

Single-scattering properties of droxtals

Ping Yang^{a,*}, Bryan A. Baum^b, Andrew J. Heymsfield^c, Yong X. Hu^b,
Hung-Lung Huang^d, Si-Chee Tsay^e, Steve Ackerman^d

^a*Department of Atmospheric Sciences, Texas A&M University, TAMU 3150, College Station, TX 77843, USA*

^b*NASA Langley Research Center, MS 420, Hampton, VA 23681, USA*

^c*National Center for Atmospheric Research, Boulder, CO 8030, USA*

^d*Cooperative Institute for Meteorological Satellite Studies, University of Wisconsin–Madison, 1225 W.
Dayton Street, Madison, WI 53706, USA*

^e*Code 913, NASA Goddard Space Flight Center, Greenbelt, MD 20771, USA*

Received 1 June 2002; accepted 2 September 2002

Abstract

Small ice crystals have been found to occur in high concentrations in high concentrations in polar stratospheric clouds and the upper portion of cirrus clouds, where temperatures are extremely low (often less than -50°C). The scattering properties of these small crystals are important to space-borne remote sensing, especially for the retrieval of cirrus properties using visible and near-infrared channels. Previous research has shown that the commonly used spherical and “quasi-spherical” approximations for these ice crystals can lead to significant errors in light scattering and radiative transfer calculations. We suggest that droxtals more accurately represent the shape of these small ice crystals. The single-scattering properties of ice droxtals have been computed at visible and infrared wavelengths using the finite-difference time domain method for size parameters smaller than 20. Further study of the optical properties of larger droxtals (size parameter greater than 20) will be carried out using an improved geometric optics method.

© 2003 Elsevier Science Ltd. All rights reserved.

Keywords: Small ice crystals; Droxtals; Optical properties

1. Introduction

In recent years, the atmospheric radiative transfer and remote sensing communities have made a concerted effort to improve the characterization of ice clouds (e.g. [1]). In particular, substantial effort has been focused on the effects of ice crystal nonsphericity on cirrus radiative characteristics. Mishchenko et al. [2] showed that the use of inappropriate ice crystal shapes, or habits, in the

* Corresponding author. Tel.: +1-979-845-4923; fax: +1-979-862-4466.

E-mail address: pyang@ariel.met.tamu.edu (P. Yang).

retrieval of cirrus optical thickness from visible wavelength reflectance measurements can lead to underestimation or overestimation of the actual optical thickness by a factor that can easily exceed 3. Because of the importance of ice crystal morphology, a number of studies have been carried out to calculate the single-scattering properties of ice crystals for various shapes [3,4], although a pristine hexagonal geometry, such as hexagonal columns, is assumed frequently for ice crystals in many applications.

Cirrus microphysical measurements conducted by Heymsfield and colleagues using balloon-borne ice crystal replicators (e.g. [5]) show that the shapes and sizes of ice crystals vary with height within midlatitude cirrus. Midlatitude cirrus tend to form in ascending air parcels where the updraft velocities are relatively low, typically less than 100 cm s^{-1} . Once formed, ice crystals tend to undergo “size sorting” and growth that lead the smallest particles to reside near cloud top and the largest particles to reside near cloud base (Fig. 1).

A generalized midlatitude cirrus cloud can be described as being composed of three layers. Small pristine ice crystals with aspect ratios (the ratio of particle length to particle diameter) of

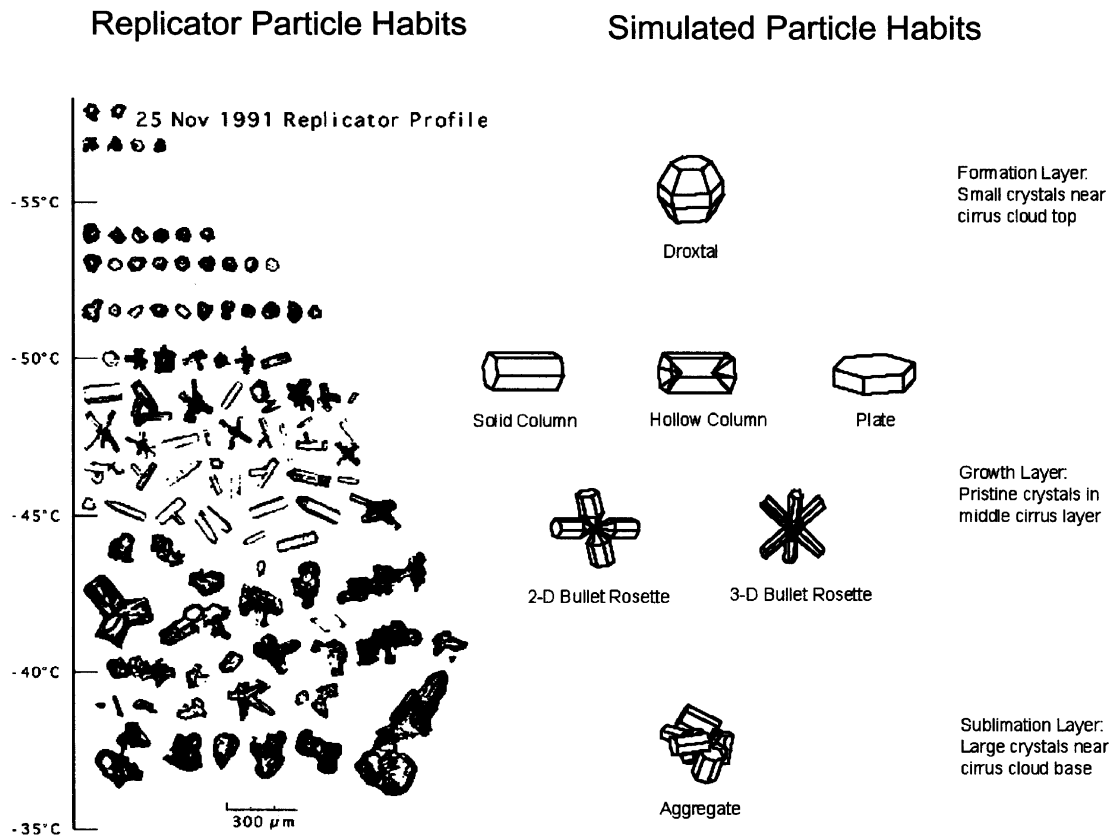


Fig. 1. (left panel) A vertical sampling of crystals obtained by a replicator on 25 November 1991 during the First ISCCP Field Experiment (FIRE, ISCCP refers to the International Satellite Cloud Climatology Project) in Coffeyville, Kansas (after Heymsfield and Iaquinta [5] with permission of the American Meteorological Society). (right panel) The ice crystal morphologies in cirrus clouds that have been suggested for light scattering and radiative transfer calculations.

approximately unity form in the uppermost portion of cirrus clouds. The small ice crystals at cloud top in the formation layer are often regarded as “quasi-spherical”, a term that is misleading in the analysis of in situ microphysical data and also in the theoretical study of the radiative properties of cirrus clouds. Identification of ice particle morphology as “quasi-spherical” leads to the common practice of applying Lorenz–Mie theory to the theoretical calculation of the optical properties of these “quasi-spherical” ice crystals. We suggest that the droxtal ice crystal shape better captures the complexity of small particle geometry as compared to spheres.

The middle layer, or growth layer, contains growing ice crystals and, for this case anyway, is dominated by pristine plates, columns and bullet rosettes. Near cloud base, the crystal population is composed primarily of irregular polycrystals or aggregates. The rounded edges of the crystals are indicative of sublimating particles. Various ice crystal geometries suggested for light scattering and radiative transfer simulations involving midlatitude cirrus cloud systems are illustrated in the right panel of Fig. 1.

Previous research has demonstrated that the modeled bidirectional reflectance of cirrus clouds, an important parameter in space-borne cloud retrieval algorithms, is highly sensitive to the geometry of the small ice crystals in the top portion of cirrus clouds [6]. Thus, there is a need to improve the accuracy of simulation of the optical properties of these small ice crystals. The intent of this study is to propose a more realistic geometry for the small ice crystals at cloud top for light scattering calculations. Second, the single-scattering properties of these ice crystals, or droxtals, are computed by the finite-difference time domain (FDTD) method. Finally, we compare and contrast the optical properties of droxtals to those of ice spheres.

2. Small ice crystals in cirrus and polar stratospheric clouds

The number concentration of ice crystals as a function of crystal maximum dimension in the uppermost portion of a midlatitude cirrus cloud observed on 5 December 1991, is illustrated in Fig. 2. The geometrical thickness of the cirrus formation layer near cloud top is approximately 1.24 km, whereas the total geometrical thickness of the cloud is 3.53 km. The temperature for the cloud layer ranges from -39°C at cloud base to -65°C at cloud top. Fig. 2 shows that there are a substantial number of ice crystals smaller than $50\ \mu\text{m}$. For the top layer of the cloud, analysis of particle morphology based on replicator images indicates that ice crystals larger than $50\ \mu\text{m}$ are mainly columns. Proper geometric identification of the small ice crystals is difficult because of insufficient resolution of the particle images. Nevertheless, we conclude that the small ice crystals are not spheres, but rather compact particles with aspect ratios that are close to unity. The blurred edges of the replicator images of small ice crystals might lead one to conclude that these small ice crystals are rounded with a “quasi-spherical” geometry. One might then treat these particles as spheres in radiative calculations, which we later demonstrate to be inappropriate.

Ohtake [7] noted in an early study that “except for ice fog crystals, we have never yet observed spherical shaped ice crystals smaller than several hundred microns in the atmosphere”. Although various observations provide evidence that many small ice crystals are not ice spheres, these particles are frequently treated as spheres in light scattering and radiative transfer calculations involved in atmospheric research. One reason for this simplification is the complexity involved in scattering calculations for ice crystals. The potential errors associated with treating ice crystals as spheres

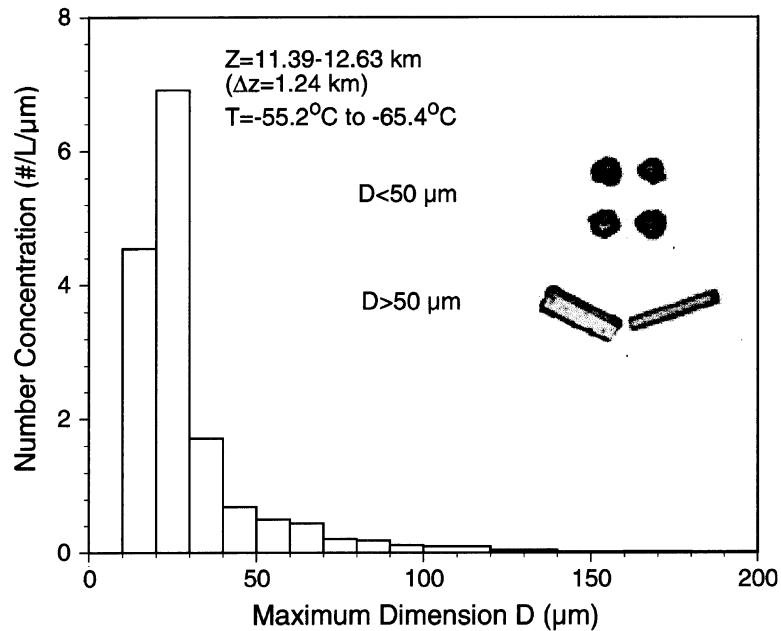


Fig. 2. Size distribution of ice crystals in top layer of a cirrus cloud observed on 5 December 1991. Data courtesy of A. J. Heymsfield, L. Miloshevich, and S. Aulenbach, National Center for Atmospheric Research.

in single-scattering and radiative transfer calculations have been investigated in a recent study by Yang et al. [6]. In that study, small ice crystals (smaller than 50 μm) in the top portions of cirrus clouds were approximated either as spheres or compact hexagons with an aspect ratio of unity. The morphologies for ice crystals larger than 50 μm were assumed to be the same in the two cases. The resultant difference of the bulk phase functions between the two treatments was significant. The use of the two phase functions to calculate the bidirectional reflectance of the cirrus cloud led to differences of (\pm)20%, depending on incidence and view geometries even for thin cirrus clouds with visible optical thickness of unity [6].

The perfect compact hexagonal geometry may be too idealistic for small ice crystals in cirrus or polar stratospheric clouds (PSCs) because the temperature at cloud top is very low (-50°C or colder). If crystals form from supercooled water droplets near -40°C , the droplets may freeze so quickly that the crystals do not have sufficient time to reach an equilibrium state for the development of normal hexagonal and rectangular faces, as pointed out by Ohtake [7]. One realistic approximation of the small ice crystal geometries may be the droxtal shape whose geometry is shown in Fig. 3. Ice droxtals have been observed in arctic ice fog [7,8]. Note that the edges of these particles in the images tend to be rounded due to insufficient instrument resolution or diffraction effects. As such, many ice crystals captured by in situ cirrus microphysical measurements, identified as “quasi-spheres”, may possibly be droxtals. The geometry of a droxtal is more complicated than for a pristine hexagonal ice crystal. For the former there are 20 faces, whereas a hexagonal ice crystal has only 8 faces. In addition, the faces of a hexagonal ice crystal tend to be more regular.

For the present light scattering computations, we assume that droxtals have maximum sphericity. According to Barrett [9] and Wadell [10,11], three independent properties, i.e. form, roundness,

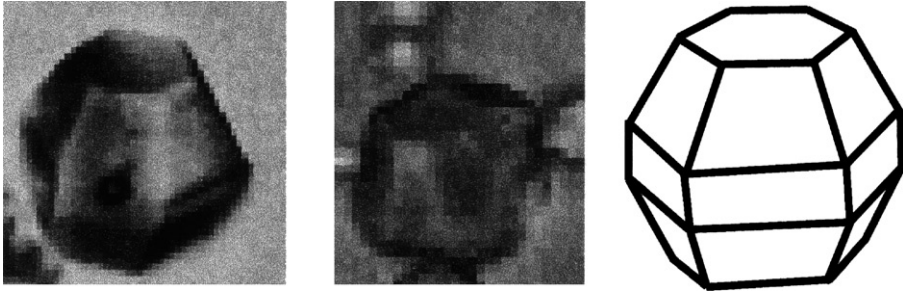


Fig. 3. Geometry of droxtals (after Ohtake [6] with permission of the American Meteorological Society).

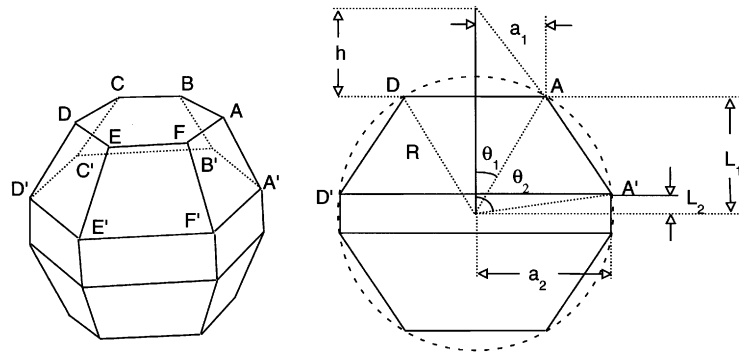


Fig. 4. The geometrical configuration of a droxtal.

and surface texture, are required to describe the external morphology of a nonspherical particle. Roundness is a large-scale property on a scale comparable to the particle dimension, and is described in terms of the sharpness of the corners where the various plates meet, as well as the convexity of the particle outline. Surface texture is a small-scale property that defines the roughness of the surface. The form is defined by the overall particle shape, often referred to as the crystal habit. Roundness and surface texture are not explicitly addressed in the present study, as we make simplifying assumption about them as described below.

Sphericity of a nonspherical particles is normally specified by the ratio of its volume, or surface area, to the corresponding property of its circumscribing sphere [11]. To maximize sphericity of a droxtal, all the vertices of the droxtal must fall on its circumscribing sphere, as illustrated in Fig. 4. Using the notation in the diagram, we have the following relationships for various parameters:

$$a_1 = R \sin \theta_1, \quad a_2 = R \sin \theta_2, \tag{1a}$$

$$L_1 = R \cos \theta_1, \quad L_2 = R \cos \theta_2, \tag{1b}$$

$$h = \frac{a_1}{(a_2 - a_1)}(L_1 - L_2), \tag{1c}$$

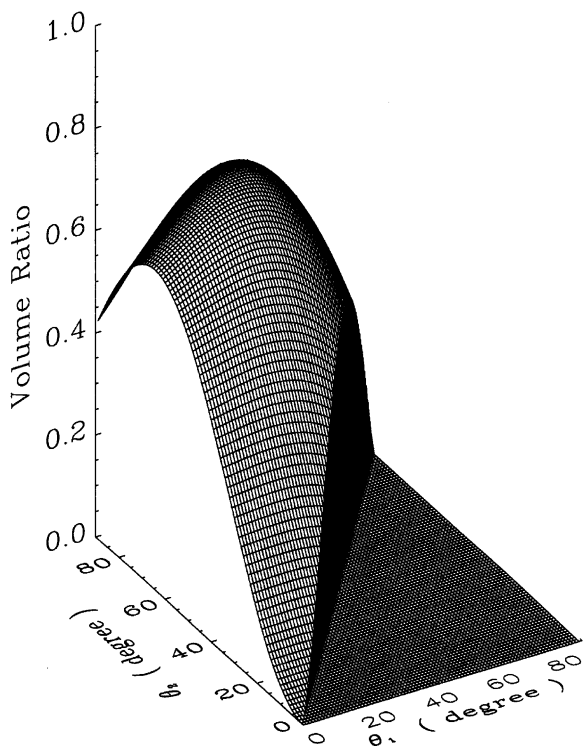


Fig. 5. The ratio of the droxtal’s volume to that of its circumscribing sphere as function of θ_1 and θ_2 .

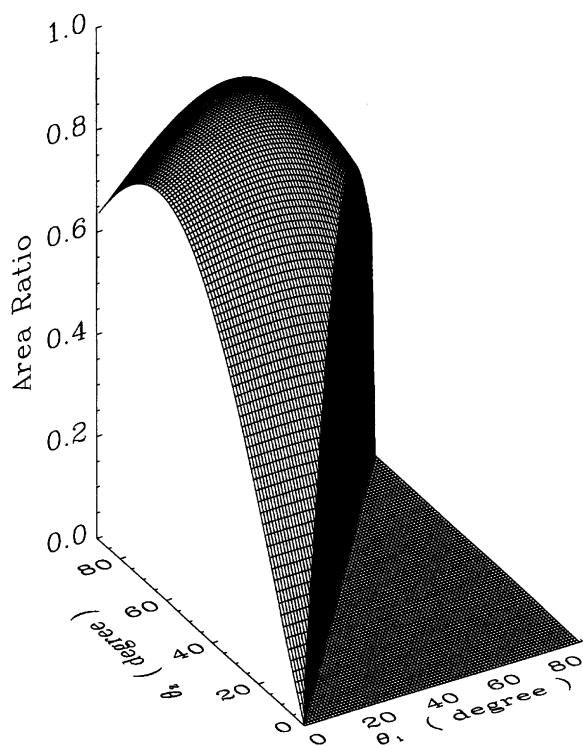


Fig. 6. Same as Fig. 4 except for the surface area ratio.

where R is the radius of the circumscribing sphere. The volume (V) and surface area (S) of the droxtal are given in terms of the parameters in Eqs. (1a)–(1c) as follows:

$$V = \sqrt{3}[(h + L_1 + 2L_2)a_2^2 - ha_1^2] \tag{2a}$$

and

$$S = 3\sqrt{3}a_1^2 + 12L_2a_2 + 6(a_1 + a_2)\sqrt{3(a_2 - a_1)^2/4 + (L_2 - L_1)^2}. \tag{2b}$$

Under the condition that all the vertices of the particle are on the same circumscribing sphere, volume and surface area of a droxtal can be completely specified by three parameters: θ_1 , θ_2 , and R . The ratio of the volume, or surface area, of a droxtal to that of its circumscribing sphere, however, is determined only by the two angular parameters θ_1 and θ_2 and is independent of R .

The ratio of the volume of a droxtal to the volume of the circumscribing sphere as a function of θ_1 and θ_2 is illustrated in Fig. 5. In the diagram, the volume ratio is not shown for the region where θ_1 is larger than θ_2 , a situation that is mathematically impossible. We find that the maximum volume ratio is 0.7233, occurring at angles of $\theta_1 = 32.35^\circ$ and $\theta_2 = 71.81^\circ$. The ratio of the droxtal’s surface area to the surface area of its circumscribing sphere is presented in Fig. 6. The maximum surface area ratio of 0.8577 occurs when $\theta_1 = 34.71^\circ$ and $\theta_2 = 72.14^\circ$. Evidently, relative to its circumscribing sphere, the droxtal possessing the maximum surface area does not possess the maximum volume. In

the present light scattering calculation, we use the droxtal geometry with the maximum sphericity in terms of volume ratio.

Surface roughness can substantially affect the scattering properties of a particle if the geometric scale of the roughness is not much smaller than incident wavelength. In the case for light scattering by large ice crystals (i.e. for size parameters within the geometric optics regime), surface roughness can reduce or smooth out the scattering peaks in phase function that correspond to halos [12]. In the present study, we focus on the scattering properties of small ice crystals with size parameters that can be handled by the FDTD method. In this case the effect of surface roughness should not be as pronounced as in the case for large size parameters. For simplicity, we ignore the effect of surface roughness and assume the faces of a droxtal are perfectly smooth.

3. Single-scattering properties of droxtals

We use the FDTD method to compute the single-scattering properties of small droxtals with size parameters less than 20. The technical details of the FDTD model used in this study are described in [13,14], and will not be reiterated here. The canonical calculations are carried out at the two wavelengths of 0.66 and 11 μm for which the refractive indices of ice are (1.3078, 1.66×10^{-8}) and (1.0925, 2.48×10^{-1}), respectively. For a given wavelength and particle size, the size parameter of a droxtal can be defined in terms of the radius of its circumscribing sphere. Since small ice crystals in the atmosphere are unlikely to have preferred orientations, we assume that droxtals are randomly oriented in space.

Phase functions at the 0.66 μm wavelength for droxtals and their circumscribing spheres with size parameters of 5, 10, and 15, where the size parameter is defined as $2\pi R/\lambda$ in which R is the radius of the droxtal circumscribing sphere, are shown in Fig. 7. The forward scattering of droxtals is reduced in magnitude from that of the circumscribing sphere. We can ascribe the reduction in forward scattering to the factor that the circumscribing spheres have larger volumes, and also larger surface areas, than the droxtals.

The phase functions for spheres have larger oscillations as a function of scattering angle than their droxtal counterparts (Fig. 7). This is especially pronounced for particles having a size parameter of 15. The oscillation of the phase function originates from the phase interference of various scattered partial waves or wave modes (e.g. [15]). For droxtals the effect associated with phase interference is lessened by averaging the phase function over particle orientations.

Phase functions for spheres and droxtals at the infrared 11- μm wavelength are presented in Fig. 8. Compared with the 0.66- μm wavelength results, the differences between the scattering properties of spheres and droxtals are largely reduced at 11- μm wavelength, primarily because of the influence of absorption within the particle. In fact, the overall patterns in the phase functions for the two particle shapes are similar. For a given nonspherical particle that possesses edges and corners, detailed geometrical information of the particle morphology is less important at longer incident wavelengths because of increasing absorption.

The extinction efficiencies, absorption efficiencies, and the asymmetry parameters associated with the phase functions in Figs. 7 and 8 are listed in Table 1. At 0.66 μm the differences between droxtal and sphere in extinction efficiencies are significant, while the differences between asymmetry parameter is less than 10% for the size parameter range that we considered. At 11 μm , the differences

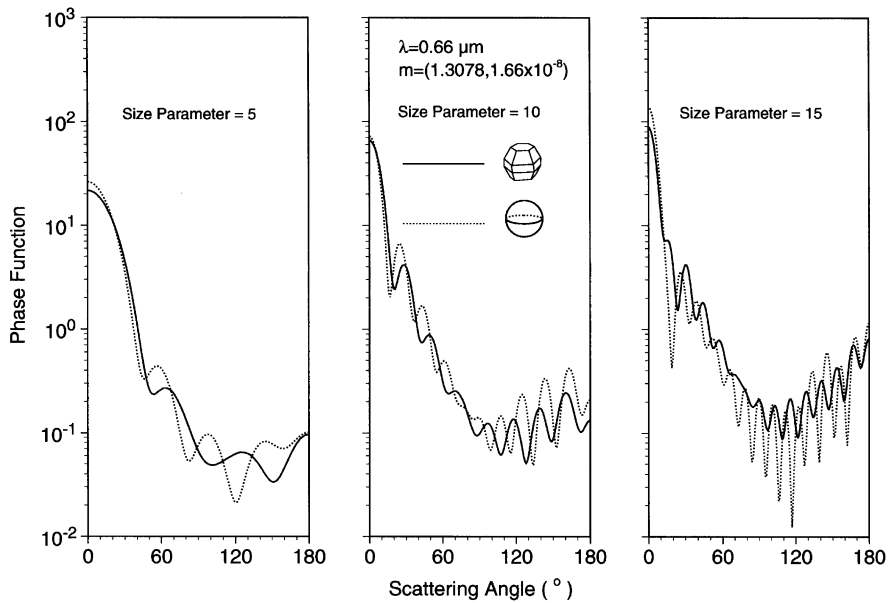


Fig. 7. The comparison of phase functions calculated for droxtals and spheres at a wavelength of 0.66 μm .

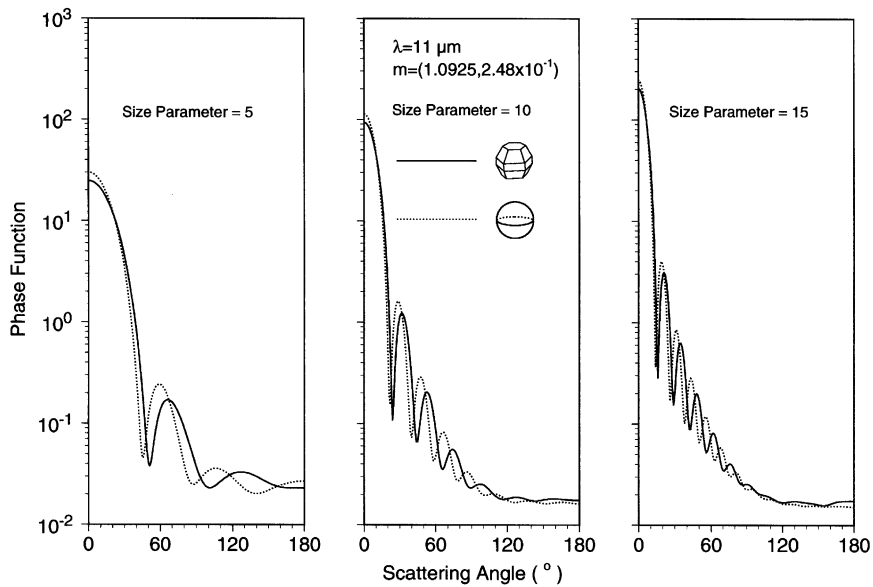


Fig. 8. Same as Fig. 7 except for a wavelength of 11 μm .

between the results for droxtal and spheres are reduced, particularly for the asymmetry parameter. However, a 10% difference in the extinction efficiency is still noted for a size parameter of 5.

Fig. 9 shows the comparison of the phase functions of droxtals, equivalent-diameter spheres, equivalent-volume spheres, and equivalent-surface-area spheres. The size parameter in the diagram

Table 1

The extinction efficiencies, absorption efficiencies, and asymmetry parameters associated with the phase functions shown in Figs. 7 and 8.

	Extinction efficiency			Absorption efficiency			Asymmetry parameter		
	Droxtal	Sphere	Difference (%)	Droxtal	Sphere	Difference (%)	Droxtal	Sphere	Difference (%)
$\lambda = 0.66 \mu\text{m}$									
$X = 5$	2.723	3.353	23.1	2.723×10^{-7}	3.463×10^{-7}	27.2	0.852	0.856	0.4
$X = 10$	2.860	2.557	-10.6	5.720×10^{-7}	7.461×10^{-7}	30.4	0.805	0.760	-6.0
$X = 15$	1.787	2.384	33.4	8.934×10^{-7}	1.118×10^{-6}	25.2	0.696	0.747	7.3
$\lambda = 11 \mu\text{m}$									
$X = 5$	1.647	1.824	10.8	1.054	1.134	7.5	0.893	0.905	1.4
$X = 10$	1.936	2.082	7.5	1.065	1.126	5.7	0.947	0.950	0.4
$X = 15$	1.995	2.118	6.2	1.044	1.093	4.6	0.959	0.960	0.2

Taking the asymmetry factor (g) as an example, the relative difference is defined as $(g_{\text{droxtal}} - g_{\text{sphere}})/g_{\text{droxtal}}$.

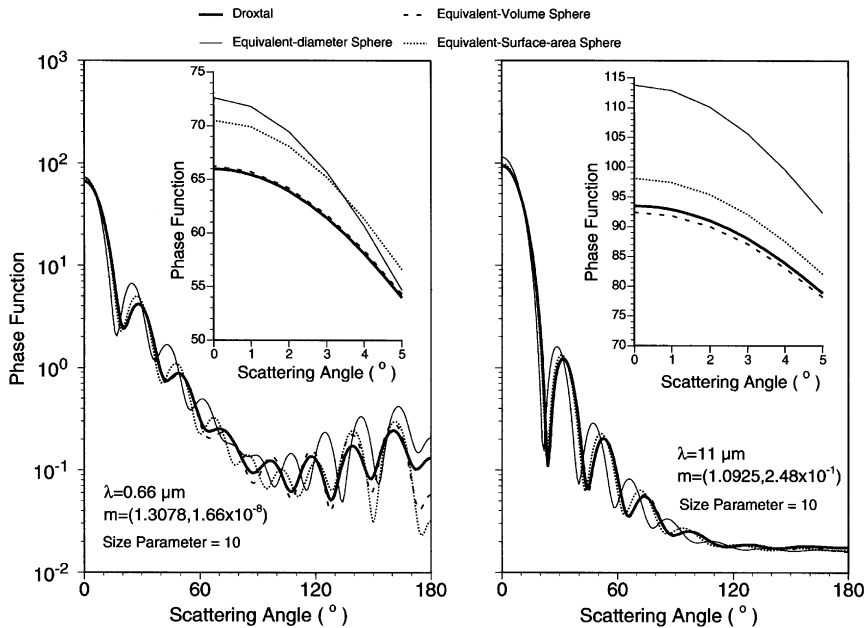


Fig. 9. The comparison of phase functions of droxtals, equivalent-diameter sphere, equivalent-volume sphere, and equivalent-surface-area sphere at 0.66- and 11- μm wavelengths.

is specified with respect to the circumscribing sphere, or the equivalent-surface-area sphere. At a wavelength of 0.66 μm , substantial differences are noted between the results for droxtals and spheres regardless of the definition of equivalent spheres, in particular, in the backscattering direction. It can be expected that the nonsphericity effect of small ice crystals can be significant in retrieving cirrus or

PSC properties based on lidar (normally operated at 0.532 and 1.064 μm wavelengths) backscattering returns. At a wavelength of 11 μm , the phase function of the equivalent-volume sphere is close to that of the droxtal. The size distribution of ice crystals is often specified with respect to the maximum dimension of particles. Thus, it is critical to calculate properly the volume of nonspherical ice crystals if one applies Lorenz–Mie theory to light scattering computation for small ice crystals at infrared wavelengths.

The present light scattering computations are limited to small ice crystals because the FDTD method is computationally inefficient in terms of computer CPU and memory requirements. For a size parameter of 15, the diameters of the droxtals are approximately 3.1 and 52 μm for wavelengths of 0.66 and 11 μm , respectively. For a droxtal with a radius of 25 μm , the size parameter of the particle is 238 at a wavelength of 0.66 μm . This size parameter is beyond the computing limits of currently available exact light scattering models. Thus, to fully understand the scattering characteristics of droxtals at visible wavelengths, other scattering computational methods, such as the geometric optics ray-tracing technique, are needed.

4. Conclusions

Droxtals may provide a realistic representation of small nonspherical ice crystals that exist in extremely cold cirrus and polar stratospheric clouds. The scattering properties of droxtals have been calculated using the FDTD method for size parameters less than 20. Substantial differences in single-scattering properties are noted between spheres and droxtals. At 0.66 μm the forward peak in the phase function for droxtals is much reduced from that calculated for ice spheres with the same diameter. Differences in extinction efficiencies between spheres and droxtals are also significant at visible wavelengths, while differences at 11 μm are not as pronounced due to increased absorption within the ice particles. To gain a complete set of the scattering properties of droxtals over a physically representative size range, the geometric optics method could be applied to them for larger size parameters. Alternatively, other techniques, such as the spheroidal geometry approach of Liu and Mishchenko [16], are useful in ascertaining the optical properties of small ice crystals in cirrus and polar stratospheric clouds.

Acknowledgements

This study was supported by research grants NAG-1-02002 and NAG5-11374 from the NASA Radiation Sciences Program managed by Dr. Donald Anderson, as well as GIFTS-IOMI MURI project. The authors thank Dr. Q. Wu for help with graphics.

References

- [1] Liou KN, Takano Y, Yang P. Light scattering and radiative transfer in ice crystal clouds: applications to climate research. In: Mishchenko MI, Hovenier JW, Travis LD, editors. *Light scattering by nonspherical particles: theory, measurements and applications*. San Diego: Academic Press, 1999.
- [2] Mishchenko MI, Rossow WB, Macke A, Lacis AA. Sensitivity of cirrus cloud albedo, bidirectional reflectance and optical thickness retrieval accuracy to ice particle shape. *J Geophys Res* 1996;101:16973–85.

- [3] Macke A, Mueller J, Raschke E. Scattering properties of atmospheric ice crystals. *J Atmos Sci* 1996;53:2813–25.
- [4] Yang P, Liou KN, Wyser K, Mitchell D. Parameterization of the scattering and absorption properties of individual ice crystals. *J Geophys Res* 2000;105:4699–718.
- [5] Heymsfield AJ, Iaquinta J. Cirrus crystal terminal velocities. *J Atmos Sci* 2000;57:916–38.
- [6] Yang P, Gao BC, Baum BA, Wiscombe WJ, Hu YX, Nasiri SL, Soulen PF, Heymsfield AJ, McFarquhar GM, Miloshevich LM. Sensitivity of cirrus bidirectional reflectance to vertical inhomogeneous of ice crystal habits and size distributions for two moderate-resolution imaging spectroradiometer (MODIS). *J Geophys Res* 2001;106:17267–91.
- [7] Ohtake T. Unusual crystal in ice fog. *J Atmos Sci* 1970;27:509–11.
- [8] Thuman WC, Robinson E. Studies of Alaskan ice-fog particles. *J Meteor* 1954;11:151–6.
- [9] Barrett PJ. The shape of rock particles, a critical review. *Sedimentology* 1980;27:291–303.
- [10] Wadell H. Volume, shape and roundness of rock particles. *J Geol* 1932;40:443–51.
- [11] Wadell H. Sphericity and roundness of rock particles. *J Geol* 1933;41:310–31.
- [12] Yang P, Liou KN. Single-scattering properties of complex ice crystals in terrestrial atmosphere. *Contr Atmos Phy* 1998;71:223–48.
- [13] Yang P, Liou KN. Finite-difference time domain method for light scattering by small ice crystals in three-dimensional space. *J Opt Soc Amer A* 1996;13:2072–85.
- [14] Yang P, Liou KN, Mishchenko MI, Gao BC. Efficient finite-difference time-domain scheme for light scattering by dielectric particles: application to aerosols. *Appl Opt* 2000;39:3727–37.
- [15] van de Hulst HC. *Light scattering by small particles*. New York: Wiley, 1957.
- [16] Liu L, Mishchenko MI. Constraints on PSC particle microphysics derived from lidar observations. *JQSRT* 2001;70:817–31.